



High expression of the *ANXA3* gene promotes immune infiltration and improves tumor prognosis in ovarian serous carcinoma using bioinformatics analyses

De-Qiang Li¹, Mao Lin², Zeinab Abdelrahman³

¹Department of General Medicine, The First Affiliated Hospital, College of Medicine, Zhejiang University, Hangzhou, China; ²Department of Rehabilitation Medicine, The First Affiliated Hospital of Zhejiang University, Hangzhou, China; ³Department of Neurobiology and Department of Rehabilitation Medicine, First Affiliated Hospital, Zhejiang University School of Medicine, Hangzhou, China

Contributions: (I) Conception and design: DQ Li; (II) Administrative support: Z Abdelrahman; (III) Provision of study materials or patients: M Lin; (IV) Collection and assembly of data: DQ Li; (V) Data analysis and interpretation: DQ Li, Z Abdelrahman; (VI) Manuscript writing: All authors; (VII) Final approval of manuscript: All authors.

Correspondence to: Zeinab Abdelrahman. Department of Neurobiology and Department of Rehabilitation Medicine, First Affiliated Hospital, Zhejiang University School of Medicine, Hangzhou 310003, China. Email: zeinabmohamed86@yahoo.com.

Background: Annexin A3 (*ANXA3*) expression change is related to tumor cell proliferation and might serve as a novel diagnostic and prognostic biomarker for cancer. However, its roles and mechanisms in ovarian serous cystadenocarcinoma (OV) have not yet been elucidated. This study aimed to investigate *ANXA3* expression in OV, its association with immune infiltrates, and its prognostic roles in OV.

Methods: The clinical data and gene expression profiles of 379 patients (189 with low *ANXA3* expression and 190 with high *ANXA3* level) with an OV diagnosis confirmed by histopathological examination were downloaded from The Cancer Genome Atlas database (<https://portal.gdc.cancer.gov>). The survival rate and expected survival time were used to measure disease prognosis. Survival curves were generated using the Kaplan-Meier method. Cox regression and a nomogram prediction model were used to analyze the relationship between *ANXA3* and the survival rate. Logistic regression was used to analyze the relationship between clinicopathological features and *ANXA3* expression. Protein-protein interactions among *ANXA3* relevant proteins were established using the Search Tool for the Retrieval of Interacting Genes/Proteins (STRING) database. The signaling pathways interacting with *ANXA3* were analyzed using Gene Ontology (GO) and Kyoto Encyclopedia of Genes and Genomes (KEGG) enrichment analyses.

Results: High *ANXA3* expression significantly correlated with lymph node infiltration (odds ratio =0.448, P=0.025) and overall favorable survival (hazard ratio =0.69, P=0.011). The Federation International of Gynecology and Obstetrics stages, primary therapy outcome, age, and residual tumor might serve as independent prognostic factors, whereas the *ANXA3* levels could not independently predict OV prognosis. *ANXA3* expression negatively and statistically (P<0.05) correlated with lymphatic invasion in Th17 cells, T follicular helper (TFH) cells, and T effector memory cells. The GO/KEGG pathway enrichment analysis confirmed the involvement of three signaling pathways in controlling the interaction of extracellular vesicles with *ANXA3*.

Conclusions: High *ANXA3* expression may contribute to tumor inhibition and a favorable prognosis to a certain extent by promoting the infiltration of TFH cells and Th17 lymphocytes or acting on extracellular vesicles inducing a stronger T-cell-mediated immunity against tumor cells.

Keywords: Annexin A3 (*ANXA3*); immune infiltrates; ovarian serous cystadenocarcinoma (OV); prognosis

Submitted Jul 11, 2022. Accepted for publication Sep 02, 2022.

doi: 10.21037/atm-22-3726

View this article at: <https://dx.doi.org/10.21037/atm-22-3726>

Introduction

Ovarian serous carcinoma (OV) is a serious, aggressive, and deadly gynecological carcinoma associated with a high recurrence rate, metastatic ability, and mortality and is resistant to conventional therapy (1). No effective method is available for early screening and diagnosis of OV. About 70% of patients are diagnosed in the advanced stage, and the 5-year survival rate is <25% for patients with stage III or IV OV (2). Although immunotherapy has recently been indicated for personalized treatment, the prognosis of advanced OV is still poor. Immune cells (3), mesenchymal cells (4), endothelial cells (5), inflammatory mediators (6), and extracellular matrix molecules contribute to the tumor microenvironment and dynamically regulate the immune response process. However, identifying immune-related genes that mediate OV prognosis may reveal new targets for OV immunotherapy. To improve the prognosis of OV, various predictive immune related biomarkers have been identified for better personalized treatments like Mesothelin (7), SLFN11 (8), B7-H4 and IDO1 (9) and so on. The new biomarkers need further verification due to some limitations like species difference, small sample size and other reasons. Bioinformatics research can often draw more accurate results based on large sample data in OV sample chip detect. Recent studies have shown that annexin A3 (*ANXA3*) gene expression is related to tumor aggressiveness and drug resistance (10). Few studies have reported on OV characteristics and therapeutic outcomes, and the role of *ANXA3* in prognosis and immune infiltration in OV remains unclear. *ANXA3* is a member of the annexin family of proteins and has 36-kDa and 33-kDa isoforms and closely related calcium (Ca^{2+})- and lipid-binding proteins. These are found at various intra- and extracellular locations, including human cumulus oophorus cells (11), and interact with a broad range of membrane lipids and proteins. Upregulation of *ANXA3* expression in tumor tissues has been found to be closely associated with cell proliferation, migration, and apoptosis (12) via the phosphatidylinositol-3 kinase/protein kinase B (13), nuclear factor- κ B (14), c-Jun (15), extracellular signal-regulated kinase, and hypoxia-inducible factor-1 signaling (16) pathways. These findings indicate that *ANXA3* may serve as a novel diagnostic and prognostic biomarker for early tumor detection and population risk screening (17). There is now an abundance of published medical data available for multifactor regression modeling and updated prediction analysis, allowing progress with high validation in medical research (18). Consequently, this

study developed an *ANXA3* gene-based signature index to identify specific immune-related prognostic biomarkers to help find better predictive and therapeutic targets to improve the prognosis of OV patients. We present the following article in accordance with the TRIPOD reporting checklist (available at <https://atm.amegroups.com/article/view/10.21037/atm-22-3726/rc>).

Methods

Data acquisition and processing

Patient datasets, with gene expression profiles and paired clinical information, were downloaded from The Cancer Genome Atlas (<https://portal.gdc.cancer.gov>) to verify the expression and prognostic impact of *ANXA3* in OV based on the GPL570 platform tested by Affymetrix Human Genome U133 Plus 2.0 Array. Totally, the gene expression profile of 379 patients confirmed by histopathological examination with clinicopathological information (189 with low *ANXA3* expression and 190 with high *ANXA3* expression) were employed in the research (Table 1). All the patients had been administered at least one treatment of chemotherapy, radiotherapy or hormone therapy except surgery. Robust multi-array average method (19) was used with default options (with background correction, quantile normalization, and log transformation) to normalize raw data from batches by R/Bioconductor's affy package. Using Xiantao Academic online platform (<https://www.xiantao.love>) to perform the bioinformatics and multivariate analysis to determine the role of *ANXA3* on OV. This online platform comprises multiple modules, including basic mapping, difference analysis, functional clustering, interactive network, clinical significance, and other analysis modules. Bioinformatics analyses include gene expression difference, immune infiltrating lymphocyte subtype cell expression, Gene Ontology (GO) and Kyoto Encyclopedia of Genes and Genomes (KEGG) enrichment and protein-protein interactions (PPIs) and were performed according to the self-contained software system. Indicators for prognostic evaluation include screening predictors, Kaplan-Meier survival curve and survival nomogram. The correlation of *ANXA3* RNA sequencing with the clinicopathological information on the prognosis of OV was evaluated by Origin 9.1 (OriginLab Corporation, USA), a standard scientific data analysis and graphing software, to obtain a visible survival curve. The "interactive network" module of Xiantao Academic was used to further determine

Table 1 Demographic characteristics of the included datasets (chi-square test)

Characteristic	Low level of <i>ANXA3</i>	High level of <i>ANXA3</i>	P
Patients (n)	189	190	–
FIGO stage, n (%)			0.330
Stage I	0 (0.0)	1 (0.3)	
Stage II	8 (2.1)	15 (4.0)	
Stage III	149 (39.6)	146 (38.8)	
Stage IV	30 (8.0)	27 (7.2)	
Primary therapy outcome, n (%)			0.898
Progressive disease	14 (4.5)	13 (4.2)	
Stable disease	11 (3.6)	11 (3.6)	
Partial remission	23 (7.5)	20 (6.5)	
Complete response	103 (33.4)	113 (36.7)	
Race, n (%)			0.401
Asian	6 (1.6)	6 (1.6)	
Black or African American	9 (2.5)	16 (4.4)	
White	164 (43.3)	164 (43.3)	
Age (years), median (IQR)	59.0 (51.0–69.0)	58.5 (50.25–67.0)	0.426

ANXA3, annexin A3; FIGO, International Federation of Gynecology and Obstetrics; IQR, interquartile range.

the relationships between *ANXA3* expression and 23 tumor-infiltrating immune cells, including T helper cells, natural killer (NK) cells, Th1 and Th2 cells, macrophages, mast cells, T gamma delta (Tgd) cells, CD8⁺ T cells, plasmacytoid dendritic cells (pDCs), NK CD56 bright cells, NK CD56 dim cells, B cells, immature dendritic cells (iDCs), regulatory T cells (Treg), activated dendritic cells (aDCs), dendritic cells, T central memory (Tcm) cells, T effector memory (Tem) cells, T cells, cytotoxic cells, neutrophils, eosinophils, T follicular helper (TFH) cells, and Th17 cells. Three ovarian tumor datasets containing 1,691 samples were downloaded from the Gene Expression Omnibus repository to obtain the network of interacting proteins. The interactome consisted of the gene regulatory pathways to determine cellular behavior. PPIs among *ANXA3* relevant proteins were established using the Search Tool for the Retrieval of Interacting Genes/Proteins (STRING) database. The signaling pathways of *ANXA3* interactions were obtained by GO/KEGG enrichment analyses. The study was conducted in accordance with the Declaration of Helsinki (as revised in 2013).

Statistical analysis

Data were expressed as the median (interquartile range) or means \pm standard deviation (SD) for continuous variables and the rate/constituent ratio for frequency distribution and categorical variables using Origin 9.1 software for statistical analysis. After multiple logistic regression analysis, the Kaplan-Meier plotter was used for the survival data analysis. Correlations between clinical characteristics and *ANXA3* expression were calculated using multiple regression analysis. The Cox logistic regression analysis was used to identify the overall survival-related clinical characteristics of patients with OV. The correlation analysis between *ANXA3* gene expression and immune cell infiltration was assessed using Spearman's R. A P value <0.05 indicated a statistically significant difference.

Results

Survival outcomes and multivariate analysis

The results indicated that the expression of *ANXA3* was

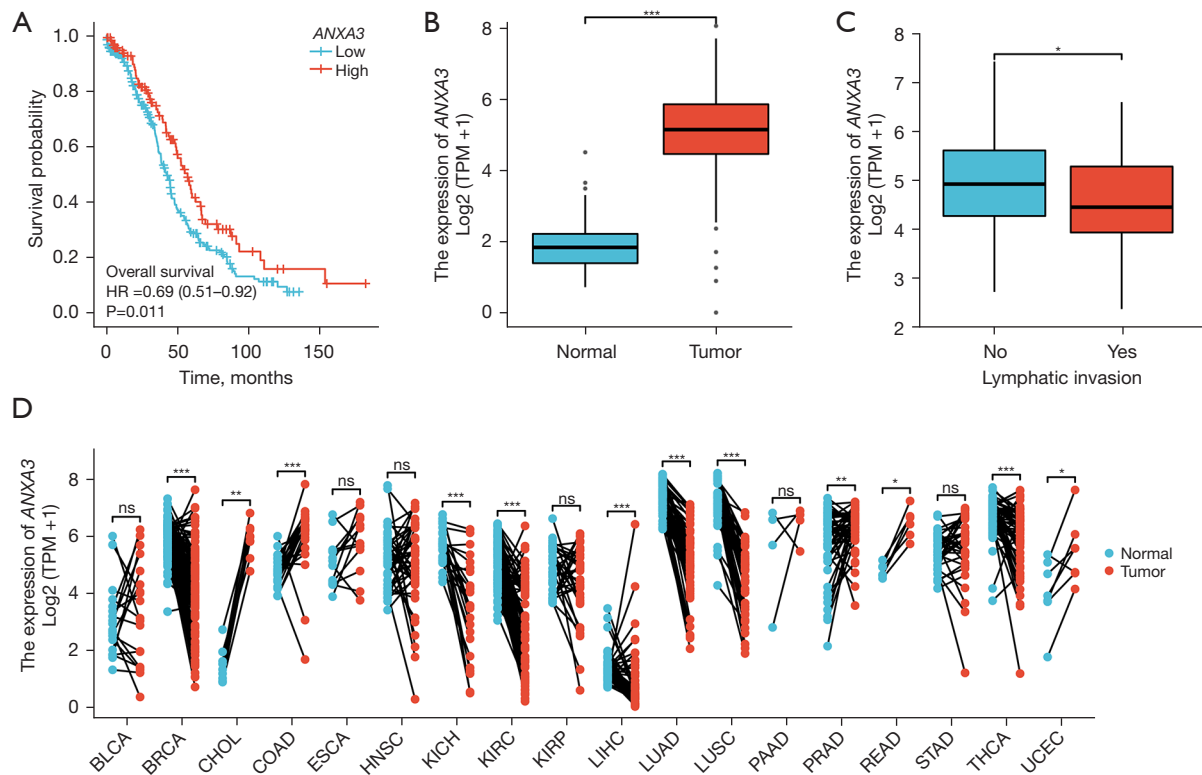


Figure 1 Survival outcomes and expression differences detected by gene expression profiling interactive analysis. (A) Increased *ANXA3* gene expression was associated with favorable outcomes. (B) Differential expression of *ANXA3* in healthy populations (normal) and patients with ovarian serous carcinoma (tumor). (C) Different expressions of *ANXA3* in different lymphatic invasions (no or yes). (D) Differential expressions of *ANXA3* in other tumor populations, including BLCA, BRCA, CHOL, COAD, ESCA, HNSC, KICH, KIRC, KIRP, LIHC, LUAD, LUSC, PAAD, PRAD, READ, STAD, THCA, and UCEC tested by paired data comparison. *, $P < 0.05$; **, $P < 0.01$; ***, $P < 0.001$. BLCA, bladder urothelial carcinoma; BRCA, breast cancer; CHOL, cholangiocarcinoma; COAD, colon adenocarcinoma; ESCA, esophageal carcinoma; HNSC, head and neck squamous cell carcinoma; KICH, kidney chromophobe; KIRC, kidney renal clear cell carcinoma; KIRP, kidney renal papillary cell carcinoma; LIHC, liver hepatocellular carcinoma; LUAD, lung adenocarcinoma; LUSC, lung squamous cell carcinoma; PAAD, pancreatic adenocarcinoma; PRAD, prostate adenocarcinoma; READ, rectum adenocarcinoma; STAD, stomach adenocarcinoma; THCA, thyroid carcinoma; UCEC, uterine corpus endometrial carcinoma; HR, hazard ratio; *ANXA3*, annexin A3; TPM, transcript per million; ns, no statistical significance.

abnormal in patients with OV. The upregulated *ANXA3* expression level significantly correlated with a good overall survival [Figure 1A, hazard ratio (HR) = 0.69, $\chi^2 = 6.48$, $P = 0.011$] and a markedly high *ANXA3* expression was present in OV tissues compared with normal tissues [Figure 1B, 1.83 (1.387–2.21) vs. 5.138 (4.454–5.849), $t = 589.5$, $P < 0.001$]. As shown in Figure 1C, unpaired-sample data studies show that the expression level of *ANXA3* significantly increased in patients with lymphatic invasion compared with those with non-lymphatic invasion (4.947 ± 0.983 vs. 4.588 ± 0.983 , $t = 2.08$, $P = 0.039$). Due to the lack of paired OV data and the possibility of decreased

expression of *ANXA3* in any other tumors, the differences in *ANXA3* RNAseq data were detected using the Wilcoxon signed-rank test (Figure 1D). Compared with matched healthy controls, the *ANXA3* expression in tumor tissues decreased significantly in breast cancer (BRCA, $n = 112$, $P < 0.001$), kidney chromophobe (KICH, $n = 23$, $P < 0.001$), kidney renal clear cell carcinoma (KIRC, $n = 72$, $P < 0.001$), liver hepatocellular carcinoma (LIHC, $n = 50$, $P < 0.001$), lung adenocarcinoma (LUAD, $n = 57$, $P < 0.001$), lung squamous cell carcinoma (LUSC, $n = 49$, $P < 0.001$), and thyroid carcinoma ($n = 58$, $P < 0.001$) and markedly increased in other tumor tissues, including cholangiocarcinoma

Table 2 Relationship between *ANXA3* and clinical features (multiple regression analysis)

Characteristics	Total (n)	Odds ratio (95% CI)	P
FIGO stage (stages III and IV vs. stages I and II)	376	0.483 (0.192–1.128)	0.103
Primary therapy outcome (CR vs. PD, SD, and PR)	308	1.197 (0.734–1.954)	0.471
Race (White vs. Asian, Black, or African American)	365	0.682 (0.336–1.351)	0.277
Age (>60 vs. ≤60 years)	377	0.890 (0.593–1.335)	0.574
Histologic grade (G3 and G4 vs. G1 and G2)	369	0.579 (0.303–1.079)	0.089
Anatomic neoplasm subdivision (bilateral vs. unilateral)	357	0.778 (0.489–1.231)	0.285
Venous invasion (yes vs. no)	105	0.467 (0.207–1.031)	0.062
Lymphatic invasion (yes vs. no)	149	0.448 (0.219–0.897)	0.025
Residual tumor (RD vs. NRD)	335	0.914 (0.533–1.563)	0.743
Tumor status (with tumor vs. tumor free)	337	1.098 (0.651–1.853)	0.726

ANXA3, annexin A3; FIGO, International Federation of Gynecology and Obstetrics; PD, progressive disease; SD, stable disease; PR, partial remission; CR, complete response; RD, residual disease; NRD, no residual disease.

(CHOL, $n=9$, $P=0.004$), colon adenocarcinoma (COAD, $n=41$, $P<0.001$), prostate adenocarcinoma (PRAD, $n=52$, $P=0.007$), and rectum adenocarcinoma (READ, $n=9$, $P=0.004$). In addition, multiple regression analysis (Figure 2A) was performed to detect the association between *ANXA3* expression levels and OV clinical variables. The results indicated that the Federation International of Gynecology and Obstetrics (FIGO) stage ($HR = 2.495$, $P=0.037$), primary therapy outcome including stable disease (SD) and complete response (CR) ($HR_{SD} = 0.441$ and $HR_{CR} = 0.152$, all $P<0.05$), age ($HR = 1.355$, $P=0.021$), and residual tumor ($HR = 2.313$, $P<0.001$) could be used as independent prognostic factors, whereas the *ANXA3* expression level could not independently predict OV prognosis ($HR = 0.901$, $P=0.430$). Using the nomogram prediction model, multiple prediction indexes were integrated (Figure 2A), and then the segmentation levels with scales were converted into weighted standard scores. In the end, the total survival period was predicted to be 2.25 years from initial OV diagnosis, and the overall 1-year survival rate in all patients was calculated to be 80%, with a total weighted score of 173 points (Figure 2B).

Association between *ANXA3* gene expression and clinicopathological variables

The *ANXA3* gene could not act as an independent predictor of OV, suggesting that *ANXA3* might interact with other clinical characteristics and be beneficial to the prognosis of

OV. Hence, this study investigated the associations between *ANXA3* levels with the FIGO stage, primary therapy outcome, race, age, histologic grade, anatomic neoplasm subdivision, venous or lymphatic invasion, residual tumor, and tumor status. As shown in Table 2, a low expression of *ANXA3* correlated significantly with lymphatic invasion ($OR = 0.448$, $P=0.025$).

Relationship between *ANXA3* gene expression and tumor-infiltrating immune cells

This study indicated that *ANXA3* expression correlated positively with T helper cells, NK cells, Th1 cells, and Th2 cells and correlated negatively with macrophages, mast cells, Tgd cells, CD8 T cells, pDC, NK CD56 bright cells, NK CD56 dim cells, B cells, iDCs, Treg, aDCs, DCs, Tem cells, T cells, cytotoxic cells, neutrophils, eosinophils, and TFH cells. The Pearson's correlation analysis showed that the differences achieved statistical significance only in Th17 cells ($r=-0.169$, $P<0.001$), TFH cells ($r=-0.129$, $P=0.012$), and Tem cells ($r=-0.104$, $P=0.043$) (Figure 3A). The upregulation of *ANXA3* promoted the activity of NK cells and inhibited the activity of other lymphocytes, especially three lymphocyte subtypes: Th17 cells, TFH cells, and Tem cells. Additionally, the difference in *ANXA3* low and high expression in specific lymphocyte subsets (Figure 3) was analyzed using the Mann-Whitney U test (Table 3) in OV tissues to determine whether *ANXA3* expression in different lymphocyte subtypes in the specific

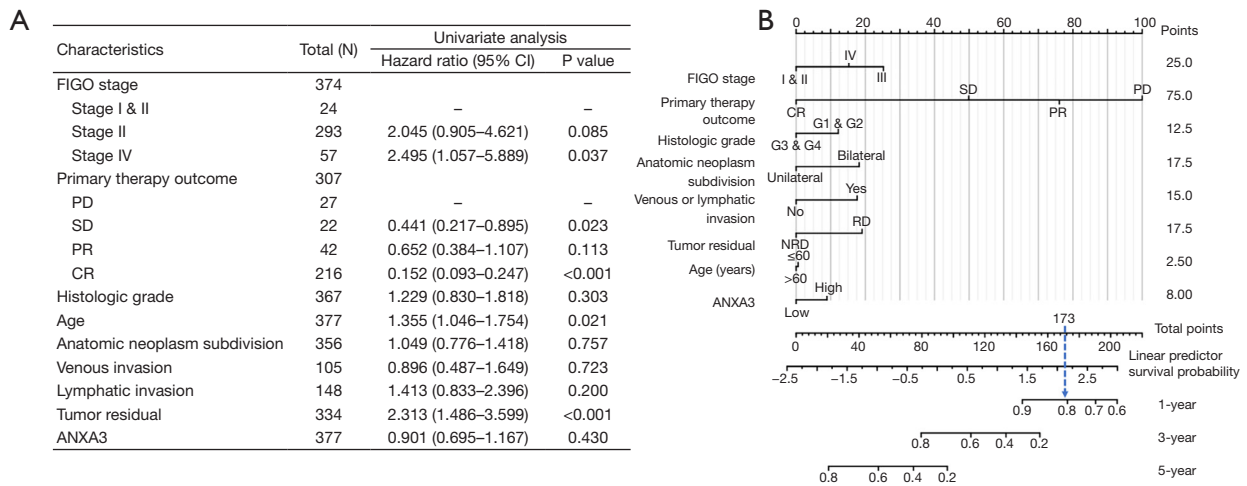


Figure 2 Multiple logistic regression analysis factors (A) and nomogram prediction for OV (B). Univariate multiple regression analysis showed that several factors, including FIGO stage (HR =2.495, P=0.037), primary therapy outcome (HR_{SD} =0.441 and HR_{CR} =0.152, all P<0.05), age (HR =1.355, P=0.021), and residual tumor (HR =2.313, P<0.001), were significantly associated with overall survival in OV, whereas the *ANXA3* level could not independently predict prognosis (HR =0.901, P=0.430). The nomogram evaluation indicated that the overall survival period was predicted to be 2.25 years from diagnosis, and the 1-year overall survival rate was almost 80%. FIGO, International Federation of Gynecology and Obstetrics; PD, progressive disease; SD, stable disease; PR, partial remission; CR, complete response; *ANXA3*, annexin A3; HR, hazard ratio; OV, ovarian serous cystadenocarcinoma; RD, residual disease; NRD, no residual disease.

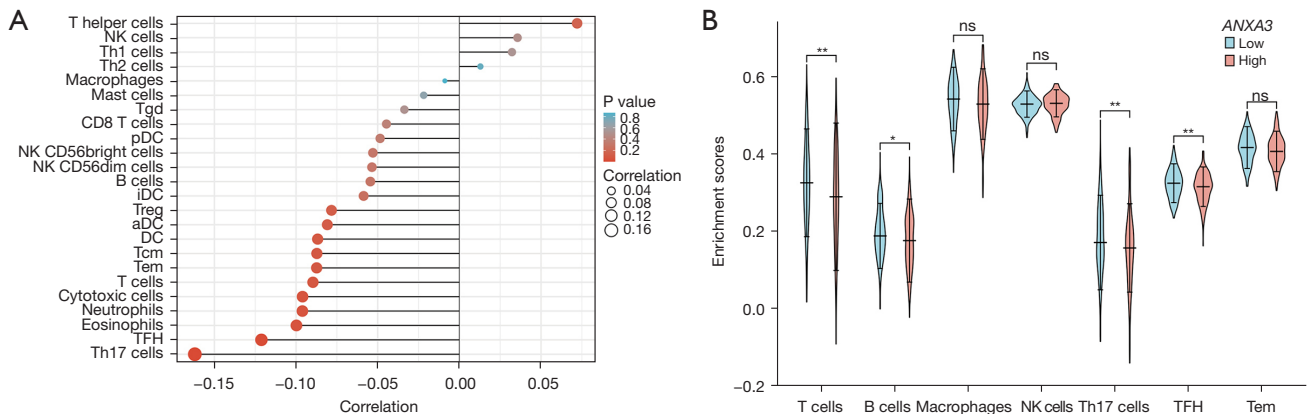


Figure 3 Relationship between *ANXA3* gene expression and cancer-infiltrating immune cell (lollipop plot) and abundance comparison results for high and low *ANXA3* expression in different cell subtypes (violin plot). (A) *ANXA3* gene expression is negatively associated with most cellular immune profiles, except T helper cells, NK cells, and Th1 and Th2 cells. (B) The Mann-Whitney *U* test revealed that among the cell subtypes involved in immune infiltration, those with low *ANXA3* expression were more enriched than those with high expression, especially in T cells, B cells, Th17 cells, and TFH cells. The differences were statistically significant (*, P<0.05; **, P<0.01). *ANXA3*, annexin A3; NK, natural killer; Tgd, T gamma delta; pDC, plasmacytoid dendritic cell; iDC, immature dendritic cell; Treg, regulatory T cells; aDC, activated dendritic cell; DC, dendritic cell; Tcm, T central memory; Tem, T effector memory; TFH, T follicular helper; ns, no statistical significance.

Table 3 Comparison of *ANXA3* high and low expression in specific lymphocyte subtypes (Mann-Whitney U test)

Lymphocyte subtypes	High (n=190)	Low (n=189)	Z	P
T cells	0.285±0.125	0.324±0.113	14,838	0.003
B cells	0.175±0.073	0.194±0.067	15,513	0.022
Macrophages	0.524±0.069	0.535±0.06	16,267	0.114
NK cells	0.527±0.026	0.524±0.025	19,507	0.146
Th17 cells	0.153±0.099	0.18±0.093	15,149	0.009
TFH cells	0.31±0.039	0.322±0.037	15,222	0.010
Tem cells	0.406±0.039	0.412±0.038	16,065	0.076

Means and standard deviation of *ANXA3* mRNA expression values in different groups. *ANXA3*, annexin A3; NK, natural killer; TFH, T follicular helper; Tem, T effector memory.

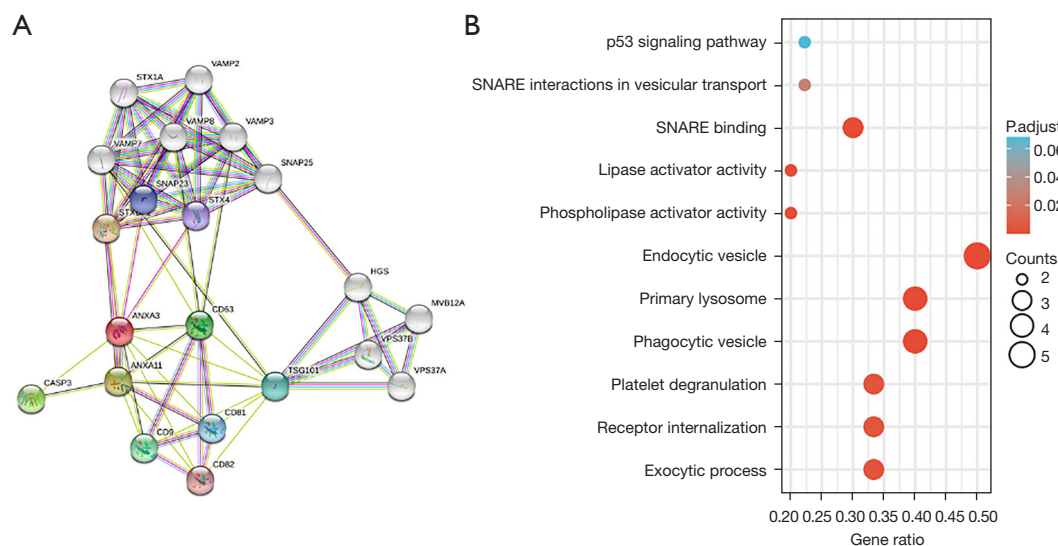


Figure 4 *ANXA3*-related protein interaction network and gene biological functional distribution in ovarian tumor. (A) Protein-protein interaction network of 21 differentially expressed proteins. The colored dot indicates a straight functional protein cluster to *ANXA3*. (B) Bubble diagram of the GO and the KEGG enrichment analysis showing differentially expressed gene-related signaling pathways. The X-axis represents different signal path descriptors. The Y-axis represents the relative intensity of the gene expression. The size and chroma of the bubble show the proportion of gene expression and adjusted P value. *ANXA3*, annexin A3; FIGO, International Federation of Gynecology and Obstetrics; GO, Gene Ontology.

location mainly increased or decreased. The results revealed marked low expression compared with high expression in T cells (0.324 ± 0.113 vs. 0.285 ± 0.125 , $P=0.003$) and B cells (0.194 ± 0.067 vs. 0.175 ± 0.073 , $P=0.022$). The same statistical results showed that low expression was more significant than high expression in Th17 cells (0.18 ± 0.093 vs. 0.153 ± 0.099 , $P=0.009$) and TFH cells (0.322 ± 0.037 vs. 0.310 ± 0.039 , $P=0.010$); no significant differences were found in NK cells ($P=0.146$), macrophages ($P=0.114$), or Tem cells ($P=0.076$).

ANXA3-related protein interaction network and GO/KEGG signaling pathway enrichment analysis

The PPI revealed the four most essential *ANXA3*-associated molecular markers of lymphatics: CD63, CD81, CD82, and CD9, and six additional functional genes: *CASP3*, *TSG101*, *STX4*, *STXBP2*, *SNAP23*, and *ANXA11* based on the differential expression (Figure 4A). The GO/KEGG analysis of *ANXA3*-related genes revealed 10 significantly

Table 4 GO/KEGG enrichment analysis results of differentially expressed genes and their innate immune functions

Ontology	ID	Description	P value	Gene ID
BP	GO:0140029	Exocytic process	6.25e-06	<i>STX4/STXBP2/SNAP23</i>
BP	GO:0031623	Receptor internalization	1.67e-05	<i>CD9/CD63/CD81</i>
BP	GO:0002576	Platelet degranulation	2.57e-05	<i>CD9/CD63/STXBP2</i>
CC	GO:0030139	Endocytic vesicle	1.96e-07	<i>ANXA11/CD9/STX4/STXBP2/SNAP23</i>
CC	GO:0045335	Phagocytic vesicle	3.91e-07	<i>ANXA11/STX4/STXBP2/SNAP23</i>
CC	GO:0005766	Primary lysosome	7.44e-07	<i>ANXA11/CD63/STXBP2/SNAP23</i>
MF	GO:0016004	Phospholipase activator activity	1.89e-05	<i>CASP3/STX4</i>
MF	GO:0060229	Lipase activator activity	2.61e-05	<i>CASP3/STX4</i>
MF	GO:0000149	SNARE binding	2.72e-05	<i>STX4/STXBP2/SNAP23</i>
KEGG	hsa04130	SNARE interactions in vesicular transport	5.73e-04	<i>STX4/SNAP23</i>
KEGG	hsa04115	p53 signaling pathway	0.003	<i>CASP3/CD82</i>

BP, biological process; CC, cellular component; MF, molecular function; GO, Gene Ontology; KEGG, Kyoto Encyclopedia of Genes and Genomes.

enriched pathways in OV. Most of the pathways were related to immune functions and response to OV (Figure 4B). Table 4 summarizes the most important sets of gene categories and their participating biological processes in OV. Among these, most of the genes belonged to the intracellular signaling cascade pathways directly participating in extracellular vesicle (EV) secretion (*SNAP23*, *STX4*, *STXBP2*, *CD9*, *CD63*, and *CD81*) or indirectly acting on the decisive promoting ion Ca^{2+} affecting the secretion of EVs through phospholipase A2/ Ca^{2+} and p53-mediated apoptosis signaling pathway (*P53* and *CASP3*), regulating the downstream cascade, except one molecule related to the pathway of the classical lymphocyte infiltration process represented by *CD82*.

Discussion

OV is one of the most common epithelial malignant tumors in the female reproductive system, accounting for about 30% of all ovarian carcinomas (20). Surgery, chemotherapy, radiotherapy, targeted therapy, biotherapy, and other treatment approaches are used after clinical diagnosis. However, it is difficult to achieve a complete cure, and more than 50% of patients die within 6 years (21). Considering the strong invasive and metastatic characteristics of OV with poor prognosis, more potent therapeutic and prognostic predictors related to the genetic, endocrine, gynecological disease, fertility, lifestyle, and other risk factors need to be

explored.

Inflammation is closely related to the occurrence and development of OV (22). To date, *ANXA3* has been found to not only maintain genomic integrity and facilitate cell proliferation and differentiation but also contributes to tumor initiation and growth. We synthesized the relevant literature and found that *ANXA3* expression was dysregulated in a large number of tumor populations, such as bladder urothelial carcinoma (23), BRCA (17), CHOL (16), COAD (24), esophageal carcinoma (25), head and neck squamous cell carcinoma (26), kidney chromophobe (27), kidney renal papillary cell carcinoma (28), hepatocellular carcinoma (29), LUAD (30), LUSC (31), pancreatic adenocarcinoma (32), PRAD (33), READ (34), stomach adenocarcinoma (25), thyroid carcinoma (35), and uterine corpus endometrial carcinoma (13). In this study, an increased *ANXA3* expression was associated with a favorable prognosis, suggesting that *ANXA3* might play a pivotal role in decreasing cancer risk in patients with OV. Additionally, a multiple logistic regression analysis was used to determine the predictors of tumor prognosis, including *ANXA3*. The results revealed that FIGO stage, primary therapy outcome, age, and residual tumor factors significantly predicted overall survival in OV, but the *ANXA3* expression level did not independently predict prognosis ($P > 0.05$). The total life span when the factors above worked together to predict overall survival was calculated to be 2.25 years after initial diagnosis, and the overall 1-year survival rate was about

80% using a nomogram evaluation. As *ANXA3* was not an independent predictor, the correlation between *ANXA3* and other independent predictors was further analyzed. The results showed that high *ANXA3* expression significantly correlated with lymphatic invasion, implying that *ANXA3* acted on local lymph infiltration and distant lymph node metastasis, thus influencing the prognosis of patients.

The process of lymphatic infiltration in tumors involves different lymphocyte subtypes and is associated with not only tumor diffusion and metastasis but also the immune response of the body to tumor cells. To date, many targeted drugs and immune cell therapies have been developed for clinical immunotherapy based on the research progress in lymphatic infiltration. This study verified the correlation between lymphocyte subsets and *ANXA3* gene expression to confirm the potential of different immune cells during lymphatic infiltration in OV. The findings revealed that *ANXA3* expression levels correlated positively with the number of T helper cells, NK cells, Th1 cells, and Th2 cells but correlated negatively with macrophages, mast cells, Tgd cells, CD8 T cells, pDCs, NK CD56 bright cells, NK CD56 dim cells, B cells, iDCs, Treg, aDCs, DCs, Tem cells, Tem cells, T cells, cytotoxic cells, neutrophils, eosinophils, TFH cells, and Th17 cells. Further, an increased *ANXA3* expression promoted the effects of NK cells and cytotoxic T lymphocyte functioning, which was beneficial to clinical immunotherapy. However, this promoting effect did not reach statistical significance. The significant correlation between *ANXA3* and lymphocyte subtypes appeared only in TFH cells, Th17 cells, and Tem lymphocyte subtypes, revealing that TFH- and Th17-cell-mediated immunity and pathology may highlight potential targets for OV therapies in the future.

TFH cells promote the survival, proliferation, and differentiation of B cells into immunoglobulin-producing cells and generate protective antibodies against various infections (36) and harmful stimulators (37). They also play a key role in inducing T-cell effectors to recruit activated cytotoxic NK and CD8⁺ T cells in tumors (38). The dysregulation of TFH cell responses in tumors is thought to be related to the recognition of immune checkpoints, such as programmed death protein-1 (PD-1), B cell lymphoma 6, C-C chemokine receptor 7, and C-X-C chemokine receptor type 5 (39). Recent studies have shown that other Th subsets, including Th1, Th2, Th9, and Treg, may become TFH cells under specific pathological conditions (40) and participate in the dynamic balance between Th1 and Th2 cells, mediating immunotoxicity and immunosuppression.

Th1, Th9, and TFH cells stimulate the antitumor immune response, while Th2 and Treg cells routinely induce immunosuppressive protumorigenic responses. Th17 cells also contribute to the delicate balance between Th1 and Th2 anti- versus pro-tumorigenic networks and play a dual role in impairing immune functions by targeting granzyme B production, a dominant marker for cytolytic CD4⁺ activity (41). Currently, the exact proportion and change in TFH and Th17 cell expression involved in lymphatic infiltration in ovarian tumor tissues, nontumor tissues, and invaded lymph nodes is unclear. This information is of great value for immunotherapy in OV and should be clarified in further research. Given the double-edged effects of *ANXA3* in lymphatic infiltration when moderately activated on the swelling of invaded tumor cells, once over activated, the lymph infiltration will produce a strong inflammatory reaction damaging normal tissue DNA (42) and its role in inducing the risk of tumor cell proliferation through a complex network of chemokines (43). This study also compared *ANXA3* expression in different lymphocyte subtypes. The results revealed that low *ANXA3* expression in TFH and Th17 cells was more predominant than high expression. This finding indicated that increased *ANXA3* expression promoted the downregulation of TFH and Th17 cells, improved lymphocyte immune infiltration, and enhanced the prognosis of patients with OV in precise patterns. This feature was consistent with the fact that a moderate immune response had a protective effect while an excessive immune response caused more damage to patients.

PPI maps help researchers determine the interacting protein genes and gain an understanding of specific signaling pathways. Using the STRING database, 10 *ANXA3*-related proteins were identified in this study: CD63, CD81, CD82, CD9, CASP3, TSG101, STX4, STXBP2, SNAP23, and ANXA11. The GO/KEGG enrichment analysis revealed three dominant specific pathways for the regulation of EV interactions with *ANXA3*: (I) the Ca²⁺ release-promoting signaling pathway represented by phospholipase A2; (II) the life cycle signaling involved in EV assembly, recognition, transportation, and reuptake processes (44); and (III) p53-mediated apoptosis. EVs are categorized into three forms: microvesicles, exosomes, and apoptotic bodies (45). In recent years, the immunobiological and functional research concerning EVs has made significant progress. For example, as the main component of oncosomes, tetraspanins (CD9 and CD81) function to cleave large cytoplasmic extensions from the cell body for constitutive EV secretion (46). CD63⁺ lysosome-related effector vesicles

contain protease. Perforin may be used by cytotoxic T lymphocytes and NK cells to fight against BRCA and also transports diverse immunomodulatory proteins, including major histocompatibility complex (MHC) classes I and II, costimulatory and adhesion molecules, enzymes, or cytokines (47). EVs transport programmed death protein-ligand 1 (PD-L1), which interacts with PD-1 and reduces CD8⁺ T-cell proliferation and promotes T-cell apoptosis, which in turn reduces the immune response and leads to large-scale tumor growth. PD-L1 also blocks Ca²⁺/soluble N-ethylmaleimide-sensitive factor attachment protein receptor complex induction and regulates exosome secretion (48). EVs carrying the CD95 ligand or tumor necrosis factor-related apoptosis-inducing ligand can induce the apoptosis of activated T cells via p53 to expose PD-L1, thereby inhibiting T-cell-mediated immunity against cancers (49). Given their convenient delivery via blood circulation and ability to cross biological barriers (50), exosomes released from chimeric antigen receptor T lymphocytes exhibit excellent potential as direct attackers in immunotherapy. These findings suggest that the interaction between *ANXA3* and EVs may affect the efficacy of immunotherapy and the prognosis of OV, although this requires further validation in subsequent studies.

This paper has some limitations. Firstly, the study aimed to identify important predictors using a multiple regression model in a multivariable analysis. However, the methodology and predictive accuracy of the model requires improvement. Secondly, only one standard data set was retrieved in this study and the limited number of cases were included also needs to expand the sample size to further strengthen the intensity in this study. In summary, increased *ANXA3* expression correlates with a favorable prognosis in OV, which may be achieved by promoting the infiltration of TFH and Th17 lymphocytes or by acting on EVs.

Conclusions

ANXA3 is responsible for the complexity of lymphatic infiltration related to OV outcomes. It induces a stronger T-cell-mediated immunity against tumor cells, implying that it can be used as an immunotherapy target.

Acknowledgments

Funding: None.

Footnote

Reporting Checklist: The authors have completed the TRIPOD reporting checklist. Available at <https://atm.amegroups.com/article/view/10.21037/atm-22-3726/rc>

Conflicts of Interest: All authors have completed the ICMJE uniform disclosure form (available at <https://atm.amegroups.com/article/view/10.21037/atm-22-3726/coif>). The authors have no conflicts of interest to declare.

Ethical Statement: The authors are accountable for all aspects of the work in ensuring that questions related to the accuracy or integrity of any part of the work are appropriately investigated and resolved. The study was conducted in accordance with the Declaration of Helsinki (as revised in 2013).

Open Access Statement: This is an Open Access article distributed in accordance with the Creative Commons Attribution-NonCommercial-NoDerivs 4.0 International License (CC BY-NC-ND 4.0), which permits the non-commercial replication and distribution of the article with the strict proviso that no changes or edits are made and the original work is properly cited (including links to both the formal publication through the relevant DOI and the license). See: <https://creativecommons.org/licenses/by-nc-nd/4.0/>.

References

- Jiang MM, Zhao F, Lou TT. Assessment of Significant Pathway Signaling and Prognostic Value of GNG11 in Ovarian Serous Cystadenocarcinoma. *Int J Gen Med* 2021;14:2329-41.
- Wang H, Ye F, Zhou C, et al. High expression of ENPP1 in high-grade serous ovarian carcinoma predicts poor prognosis and as a molecular therapy target. *PLoS One* 2021;16:e0245733.
- Communal L, Roy N, Cahuzac M, et al. A Keratin 7 and E-Cadherin Signature Is Highly Predictive of Tubo-Ovarian High-Grade Serous Carcinoma Prognosis. *Int J Mol Sci* 2021;22:5325.
- Otsuka I. Mechanisms of High-Grade Serous Carcinogenesis in the Fallopian Tube and Ovary: Current Hypotheses, Etiologic Factors, and Molecular Alterations. *Int J Mol Sci* 2021;22:4409.
- Escalona RM, Kannourakis G, Findlay JK, et al.

- Expression of TIMPs and MMPs in Ovarian Tumors, Ascites, Ascites-Derived Cells, and Cancer Cell Lines: Characteristic Modulatory Response Before and After Chemotherapy Treatment. *Front Oncol* 2021;11:796588.
6. Pietilä EA, Gonzalez-Molina J, Moyano-Galceran L, et al. Co-evolution of matrisome and adaptive adhesion dynamics drives ovarian cancer chemoresistance. *Nat Commun* 2021;12:3904.
 7. Giordano G, Ferioli E, Tafuni A. The Role of Mesothelin Expression in Serous Ovarian Carcinoma: Impacts on Diagnosis, Prognosis, and Therapeutic Targets. *Cancers (Basel)* 2022;14:2283.
 8. Winkler C, King M, Berthe J, et al. SLFN11 captures cancer-immunity interactions associated with platinum sensitivity in high-grade serous ovarian cancer. *JCI Insight* 2021;6:146098.
 9. Niu N, Shen W, Zhong Y, et al. Expression of B7-H4 and IDO1 is associated with drug resistance and poor prognosis in high-grade serous ovarian carcinomas. *Hum Pathol* 2021;113:20-7.
 10. Guo C, Li N, Dong C, et al. 33-kDa ANXA3 isoform contributes to hepatocarcinogenesis via modulating ERK, PI3K/Akt-HIF and intrinsic apoptosis pathways. *J Adv Res* 2021;30:85-102.
 11. Chermuła B, Hutchings G, Kranc W, et al. Expression Profile of New Gene Markers and Signaling Pathways Involved in Immunological Processes in Human Cumulus-Oophorus Cells. *Genes (Basel)* 2021;12:1369.
 12. Liu C, Li N, Liu G, et al. Annexin A3 and cancer. *Oncol Lett* 2021;22:834.
 13. Wu F, Yang J, Liu J, et al. Signaling pathways in cancer-associated fibroblasts and targeted therapy for cancer. *Signal Transduct Target Ther* 2021;6:218.
 14. Zhang Z, Li Z, Ma Z, et al. Annexin A3 as a Marker Protein for Microglia in the Central Nervous System of Rats. *Neural Plast* 2021;2021:5575090.
 15. Tam SY, Law HK. JNK in Tumor Microenvironment: Present Findings and Challenges in Clinical Translation. *Cancers (Basel)* 2021;13:2196.
 16. Wang F, Breslin S J P, Qiu W. Novel oncogenes and tumor suppressor genes in hepatocellular carcinoma. *Liver Res* 2021;5:195-203.
 17. Yang L, Lu P, Yang X, et al. Annexin A3, a Calcium-Dependent Phospholipid-Binding Protein: Implication in Cancer. *Front Mol Biosci* 2021;8:716415.
 18. Collins GS, Dhiman P, Andaur Navarro CL, et al. Protocol for development of a reporting guideline (TRIPOD-AI) and risk of bias tool (PROBAST-AI) for diagnostic and prognostic prediction model studies based on artificial intelligence. *BMJ Open* 2021;11:e048008.
 19. Albaradei S, Thafar M, Alsaedi A, et al. Machine learning and deep learning methods that use omics data for metastasis prediction. *Comput Struct Biotechnol J* 2021;19:5008-18.
 20. Zhang Y, Du T, Chen X. ANXA2P2: A Potential Immunological and Prognostic Signature in Ovarian Serous Cystadenocarcinoma via Pan-Carcinoma Synthesis. *Front Oncol* 2022;12:818977.
 21. Canals Hernaez D, Hughes MR, Dean P, et al. PODO447: a novel antibody to a tumor-restricted epitope on the cancer antigen podocalyxin. *J Immunother Cancer* 2020;8:e001128.
 22. Peres LC, Townsend MK, Birmann BM, et al. Circulating Biomarkers of Inflammation and Ovarian Cancer Risk in the Nurses' Health Studies. *Cancer Epidemiol Biomarkers Prev* 2021;30:710-8.
 23. Yao X, Qi X, Wang Y, et al. Identification and Validation of an Annexin-Related Prognostic Signature and Therapeutic Targets for Bladder Cancer: Integrative Analysis. *Biology (Basel)* 2022;11:259.
 24. Luparello C. Cadmium-Associated Molecular Signatures in Cancer Cell Models. *Cancers (Basel)* 2021;13:2823.
 25. Grewal T, Rentero C, Enrich C, et al. Annexin Animal Models-From Fundamental Principles to Translational Research. *Int J Mol Sci* 2021;22:3439.
 26. Chen N, He D, Cui J. A Neutrophil Extracellular Traps Signature Predicts the Clinical Outcomes and Immunotherapy Response in Head and Neck Squamous Cell Carcinoma. *Front Mol Biosci* 2022;9:833771.
 27. Zhang Y, Liu Q, Liu J, et al. Upregulated CD58 is associated with clinicopathological characteristics and poor prognosis of patients with pancreatic ductal adenocarcinoma. *Cancer Cell Int* 2021;21:327.
 28. Zhang C, Zhang W, Cui H, et al. Role of Hub Genes in the Occurrence and Development of Testicular Cancer Based on Bioinformatics. *Int J Gen Med* 2022;15:645-60.
 29. Romualdo GR, Leroy K, Costa CJS, et al. In Vivo and In Vitro Models of Hepatocellular Carcinoma: Current Strategies for Translational Modeling. *Cancers (Basel)* 2021;13:5583.
 30. Chen Q, Wang X, Hu J. Systematically integrative analysis identifies diagnostic and prognostic candidates and small-molecule drugs for lung adenocarcinoma. *Transl Cancer Res* 2021;10:3619-46.
 31. Chen C, Hou J, Yu S, et al. Role of cancer-associated fibroblasts in the resistance to antitumor therapy, and their

- potential therapeutic mechanisms in non-small cell lung cancer. *Oncol Lett* 2021;21:413.
32. Hendley AM, Rao AA, Leonhardt L, et al. Single-cell transcriptome analysis defines heterogeneity of the murine pancreatic ductal tree. *Elife* 2021;10:67776.
 33. Ruan Y, Xu H, Ji X, et al. BLM interaction with EZH2 regulates MDM2 expression and is a poor prognostic biomarker for prostate cancer. *Am J Cancer Res* 2021;11:1347-68.
 34. De P, Aske J, Dey N. Cancer-Associated Fibroblast Functions as a Road-Block in Cancer Therapy. *Cancers (Basel)* 2021;13:5246.
 35. Baagar KA, Alowainati BI. Papillary Thyroid Cancer Affecting Multiple Family Members: A Case Report and Literature Review of Familial Nonmedullary Thyroid Cancer. *Case Rep Endocrinol* 2021;2021:3472000.
 36. Schultheiß C, Paschold L, Simnica D, et al. Next-Generation Sequencing of T and B Cell Receptor Repertoires from COVID-19 Patients Showed Signatures Associated with Severity of Disease. *Immunity* 2020;53:442-455.e4.
 37. Cirelli KM, Carnathan DG, Nogal B, et al. Slow Delivery Immunization Enhances HIV Neutralizing Antibody and Germinal Center Responses via Modulation of Immunodominance. *Cell* 2019;177:1153-1171.e28.
 38. Bengsch B, Ohtani T, Herati RS, et al. Deep immune profiling by mass cytometry links human T and NK cell differentiation and cytotoxic molecule expression patterns. *J Immunol Methods* 2018;453:3-10.
 39. Onabajo OO, George J, Lewis MG, et al. Rhesus macaque lymph node PD-1(hi)CD4+ T cells express high levels of CXCR5 and IL-21 and display a CCR7(lo)ICOS+Bcl6+ T-follicular helper (Tfh) cell phenotype. *PLoS One* 2013;8:e59758.
 40. Wang W, Sung N, Gilman-Sachs A, et al. T Helper (Th) Cell Profiles in Pregnancy and Recurrent Pregnancy Losses: Th1/Th2/Th9/Th17/Th22/Tfh Cells. *Front Immunol* 2020;11:2025.
 41. Park S, Anderson NL, Canaria DA, et al. Granzyme-Producing CD4 T Cells in Cancer and Autoimmune Disease. *Immunohorizons* 2021;5:909-17.
 42. Shi F, Deng T, Mo J, et al. An Immune-Related Gene-Based Signature as Prognostic Tool in Ovarian Serous Cystadenocarcinoma. *Int J Gen Med* 2021;14:4095-104.
 43. Chen YF, Shao GC, Li J, et al. O-GlcNAcylation of Blimp-1 in Lymphocytes Inhibits Its Transcriptional Function and Is Associated with Migration and Invasion of Breast Cancer Cells. *Mol Cancer Res* 2022;20:650-60.
 44. Calvo V, Izquierdo M. Inducible Polarized Secretion of Exosomes in T and B Lymphocytes. *Int J Mol Sci* 2020;21:2631.
 45. Beck S, Hochreiter B, Schmid JA. Extracellular Vesicles Linking Inflammation, Cancer and Thrombotic Risks. *Front Cell Dev Biol* 2022;10:859863.
 46. Samuels M, Cilibrasi C, Papanastopoulos P, et al. Extracellular Vesicles as Mediators of Therapy Resistance in the Breast Cancer Microenvironment. *Biomolecules* 2022;12:132.
 47. Lettau M, Janssen O. Intra- and Extracellular Effector Vesicles From Human T And NK Cells: Same-Same, but Different? *Front Immunol* 2021;12:804895.
 48. Liu J, Peng X, Yang S, et al. Extracellular vesicle PD-L1 in reshaping tumor immune microenvironment: biological function and potential therapy strategies. *Cell Commun Signal* 2022;20:14.
 49. Sanaei M, Kavooosi F. Effects of trichostatin A on the intrinsic and extrinsic apoptotic pathway, cell viability, and apoptosis induction in hepatocellular carcinoma cell lines. *Gastroenterol Hepatol Bed Bench* 2021;14:323-33.
 50. Record M, Attia M, Carayon K, et al. Targeting the liver X receptor with dendrogenin A differentiates tumour cells to secrete immunogenic exosome-enriched vesicles. *J Extracell Vesicles* 2022;11:e12211.

(English Language Editor: D. Fitzgerald)

Cite this article as: Li DQ, Lin M, Abdelrahman Z. High expression of the *ANXA3* gene promotes immune infiltration and improves tumor prognosis in ovarian serous carcinoma using bioinformatics analyses. *Ann Transl Med* 2022;10(19):1055. doi: 10.21037/atm-22-3726